Semi-classical explanation for the dissociation control of H_2^+*

Jia Zheng-Mao(贾正茂), Zeng Zhi-Nan(曾志男)†, Li Ru-Xin(李儒新), and Xu Zhi-Zhan(徐至展)

State Key Laboratory of High Field Laser Physics, Shanghai Institute of Optics and Fine Mechanics, Chinese Academy of Sciences, Shanghai 201800, *China*

(Received 8 November 2013; revised manuscript received 18 February 2014; published online 10 June 2014)

A semi-classical model is utilized to explain the dissociation control of the hydrogen molecular ion (H_2^+). By analyzing the curve of the dissociation asymmetry parameter as a function of the time delay between the exciting and steering pulses, we find that the dissociation control is dependent not only on the peak intensity and direction of the electric field of the steering pulse, but also on the peak intensity of the exciting pulse.

Keywords: dissociation probability, hydrogen molecular ion, terahertz pulse, time-dependent Schrödinger equation

PACS: 32.80.Rm, 33.80.Rv, 42.50.Hz, 42.65.Ky **DOI:** 10.1088/1674-1056/23/8/083201

1. Introduction

Coherent control of electrons and fragments in chemical reactions and the photoelectron process has attracted much attention.[1–3] One of the main goals is to find a way to selectively break and form molecular bonds in photochemical reactions.[4] With the advent of new laser technologies, in particular the carrier envelope phase (CEP) stabilized few-cycle pulses and isolated subfemtosecond pulses, several control strategies have been proposed.[5–12]

H_2^+ is a simple molecule, and its isotopes play an important role in the theoretical and experimental studies of electron localization in the dissociation of molecules. In previous studies, many models have been utilized to explain the electron localization control during the dissociation of H_2^+ and its isotopes, including the mixture of the 1s σ_g and 2p σ_u states,[13] the interference between 2p σ_u and 3s σ_g states,[14] and the superposition of the 2p π_g and 2p π_u states.[15] The quantum coupled equations are also used to discuss the origin of the dissociation control.[16]

In this work, a CEP locked terahertz (THz) pulse[17–22] is used to steer the electron motion between the two protons of H_2^+ after an ultrashort ultraviolet (UV) laser pulse has excited the electron wave packet onto the dissociative states. Both the THz and UV pulses are linearly polarized. By controlling the peak intensity of the UV pulse and the time delay between the two pulses, an unprecedentedly high ratio to localize electrons on one of the two nuclei can be achieved,[23] more importantly, this scheme can reveal the origin of the electron localization control during H_2^+ dissociation.

2. Simulation model and the parameters of the electric fields

We use a reduced-dimensional model for the H_2^+ molecular ion in the calculation, in which the molecular axis is assumed to be parallel to the polarization direction of the two laser fields. We apply the one-dimensional (1D) non-Born–Oppenheimer time-dependent Schrödinger equation (TDSE)[24,25] which can be written as ($e = \hbar = m_e = 1$ in atomic units (a.u.), which are used throughout the paper unless otherwise stated),[25–28]

$$\mathrm{i}\frac{\partial}{\partial t}\varphi(z,R;t) = H(z,R;t)\varphi(z,R;t), \tag{1}$$

where

$$\begin{aligned} H(z,R;t) = & -\frac{1}{m_\mathrm{p}}\frac{\partial^2}{\partial R^2} + \frac{1}{R} - \left(\frac{2m_\mathrm{p}+m_\mathrm{e}}{4m_\mathrm{p}m_\mathrm{e}}\right)\frac{\partial^2}{\partial z^2} \\ & + \left(1+\frac{m_\mathrm{e}}{2m_\mathrm{p}+m_\mathrm{e}}\right) z(E_1(t)+E_2(t-\Delta t)) \\ & - [1+(z-R/2)^2]^{-1/2} - [1+(z+R/2)^2]^{-1/2}, \end{aligned} \tag{2}$$

where R is the relative internuclear distance, z is the electronic coordinate with respect to the center of mass of the two nuclei, and m_e and m_p are the electron and proton mass ($m_\mathrm{e} = 1$ and $m_\mathrm{p} = 1837$), respectively.

The UV pulse is defined as $E_2(t) = E_{20}\sin(\pi t/T_2)^2 \sin(\omega_2 t)$, where T_2 is the total length of the pulse, i.e., 7.9 fs.[29] The THz pulse is defined by the vector potential $A(t) = -E_{10}/\omega_1 \sin(\pi t/T_1)^2 \cos\omega_1 t)$, where T_1 is the total length, one cycle of the THz pulse, then $E_1(t) = -\partial A(t)/\partial t$ as shown in Fig. 1. The total simulation time is defined by t_end, which can be much longer than the THz pulse. For time beyond the total length of the THz pulse, the electric field is set

*Project supported by the National Natural Science Foundation of China (Grant Nos. 11127901, 60921004, 11134010, 11222439, 11227902, and 61108012) and the National Key Basic Research Program of China (Grant No. 2011CB808103).

†Corresponding author. E-mail: zhinan_zeng@mail.siom.ac.cn

© 2014 Chinese Physical Society and IOP Publishing Ltd

to be zero. Here Δt is the time delay between the two pulses, which is defined as the difference in set-out between two electric fields. More details can be found in Ref. [23]. The two channels of H_2^+ dissociation are defined as[16,30–32]

$$P_{\pm} = \int_{10.0}^{R_{\max}} \mathrm{d}R \int_{\pm R/2.0-5.0}^{\pm R/2.0+5.0} \mathrm{d}z \, |\varphi(z,R;t_{\mathrm{end}})|^2, \qquad (3)$$

where $R_{\max}$ corresponds to the boundary of the R-axis and $\varphi(z, R; t_{\mathrm{end}})$ is the final wave function of the system. In the simulation, $t_{\mathrm{end}} = 106.8$ fs when $P_{\pm}$, the probabilities for the electron localized on one of the protons (left $-$ or right $+$), are stable.

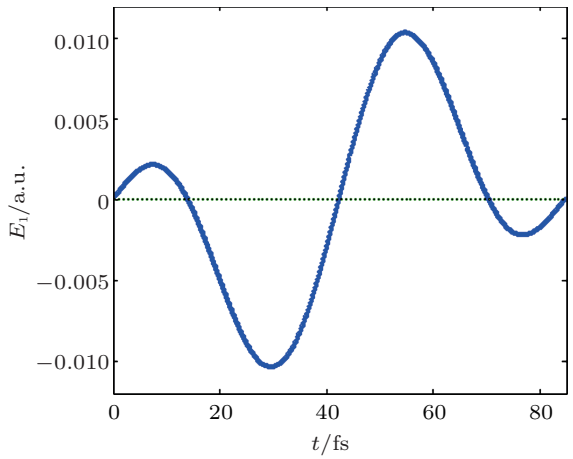


Fig. 1. (color online) The THz pulse utilized in this study.

In this simulation, the 228-nm UV pulse with an intensity of 5.0×10^{14} W/cm^2 and a pulse length T_2 of 7.9 fs is used to resonantly excite the electron wave packet onto the dissociative 2p σ_u state. Then the 25.6-μm (11.7-THz frequency) THz pulse with an intensity of 3.8×10^{12} W/cm^2 and a pulse length T_1 of 85.3 fs (one-cycle) is used to steer the electron motion. This THz pulse does not induce any further ionization. In the calculation, we set the dissociation asymmetry parameter $A = (P_+ - P_-)/(P_+ + P_-)$.

3. Simulation results and discussion

Figure 2(a) shows the variations of asymmetry parameter A, the ionization probability I, P_-, and P_+ with Δt, the time delay between the THz and UV pulses. The intensities of the THz and UV pulses are $I_1 = 3.8 \times 10^{12}$ W/cm^2 and $I_2 = 5.0 \times 10^{14}$ W/cm^2, respectively. A large dissociation asymmetry parameter $A = 0.921$ can be obtained when $\Delta t = 53.4$ fs, which corresponds to an electron localization ratio as high as 96.07% of all the dissociation events. For curve A, if we neglect the curve distortions around the delays of 20.0 fs and 34.9 fs, the whole curve is similar to that of the electric field of the THz pulse. But these distortions can reveal the origin of the asymmetric distribution of the electrons during the dissociation of H_2^+.

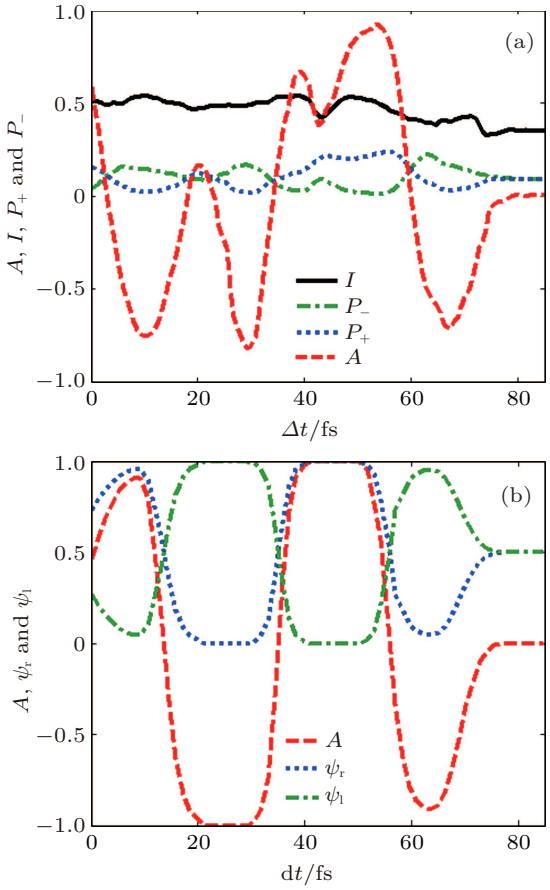


Fig. 2. (color online) (a) Results of asymmetry parameter A, ionization probability I, and $P_\pm$ versus time delay Δt, calculated from the TDSE simulation. The intensities of the THz and UV pulses are 3.8×10^{12} W/cm^2 and 5.0×10^{14} W/cm^2, respectively. (b) Results of asymmetry parameter A and the probabilities of electrons localized on the left ψ_l and right ψ_r protons versus dt, calculated from the coupled equations.

The key role that the THz pulse plays in the dissociation of the H_2^+ ion can be explained as follows. In the previous two-pulse schemes, the delayed pulse should induce single-photon coupling between the upper and lower states to achieve the electron localization. However, the photon energy of the THz pulse is too low to induce single-photon coupling between two states. So we carry on the simulation further with the following coupled equations:[23,33]

$$\begin{aligned} & \mathrm{i}\frac{\partial}{\partial t}\begin{pmatrix} \psi_g(R,t) \\ \psi_u(R,t) \end{pmatrix} \\ & = \begin{pmatrix} -\dfrac{1}{m_{\mathrm{p}}}\dfrac{\partial^2}{\partial R^2} + V_g(R) & V_{gu}(R,t) \\ V_{gu}(R,t) & -\dfrac{1}{m_{\mathrm{p}}}\dfrac{\partial^2}{\partial R^2} + V_u(R) \end{pmatrix} \\ & \times \begin{pmatrix} \psi_g(R,t) \\ \psi_u(R,t) \end{pmatrix}, \end{aligned} \qquad (4)$$

where $\psi_g(R,t)$ and $\psi_u(R,t)$ are the nuclear wave packets of 1s σ_g and 2p σ_u states, respectively, $V_g(R)$ and $V_u(R)$ denote the binding and dissociative potential curves, respectively, which can be obtained with Eq. (1), and $V_{gu}(R,t)$ is

the interaction of the external laser field with the electron. To investigate the electron localization, the nuclear wave packets on the right $\psi_{\rm r}$ and left $\psi_{\rm l}$ protons can be written, respectively, as

$$\psi_{\rm r}(R,t) = \frac{1}{\sqrt{2}}\left(\psi_g(R,t) + \psi_u(R,t)\right),$$
$$\psi_{\rm l}(R,t) = \frac{1}{\sqrt{2}}\left(\psi_g(R,t) - \psi_u(R,t)\right). \quad (5)$$

Then we can rewrite Eq. (4) with this representation as

$$\begin{aligned} {\rm i}\frac{\partial}{\partial t}\psi_{\rm r} &= \left[-\frac{1}{m_{\rm p}}\frac{\partial^2}{\partial R^2} + \frac{V_g(R)+V_u(R)}{2} + V_{gu}(R,t)\right]\psi_{\rm r} \\ &\quad + \left[\frac{V_g(R)-V_u(R)}{2}\right]\psi_{\rm l}, \\ {\rm i}\frac{\partial}{\partial t}\psi_{\rm l} &= \left[\frac{V_g(R)-V_u(R)}{2}\right]\psi_{\rm r} \\ &\quad + \left[-\frac{1}{m_{\rm p}}\frac{\partial^2}{\partial R^2} + \frac{V_g(R)+V_u(R)}{2} - V_{gu}(R,t)\right]\psi_{\rm l}. \end{aligned} \quad (6)$$

In Eq. (6), the electron jumping between the two protons $\langle\psi_{\rm r}|V_{\rm I}^{\rm rl}|\psi_{\rm l}\rangle$ is determined by the interaction potential $V_{\rm I}^{\rm rl} = [V_g(R) - V_u(R)]/2$. However, $V_{\rm I}^{\rm rl}$ is independent of the external laser field and decreases very fast (almost in the manner of e^{-R} for large R) with the increase of internuclear distance R. To investigate the role of the THz pulse, we use Eq. (4) to perform the further simulation, in which a Gaussian-type wave packet located at $R = 3.3$ a.u. (resonant with the 228-nm pulse) is pre-excited onto the dissociative state ψ_u and the steering pulse has the same wavelength as that of the THz pulse utilized in the TDSE simulation and the adjustable intensity. Figure 2(b) shows the asymmetry parameter A as a function of time delay dt between the pre-excitation of the Gaussian-type wave packet and the start of the THz pulse, which varies in a similar way to the curve A of Fig. 2(a) except that the curve is damaged around the time delays of 20.0 fs and 34.9 fs.

Figure 3 shows the time evolutions of the electron probabilities on the left and right protons under the THz pulses of different peak intensities at dt = 21.4 fs. When the peak intensity of the THz pulse is small (Fig. 3(a)), the electron probabilities on the two protons are nearly the same. With the increase of the peak intensity, more and more electrons are pulled from the right proton to the left one. When the peak intensity of the THz pulse is strong enough, most of the electrons can be localized on the left proton during the dissociation of H_2^+ (Fig. 3(d)). In these simulations, the electron probabilities on the right proton ($\int|\psi_{\rm r}|^2\,{\rm d}R$) and left proton ($\int|\psi_{\rm l}|^2\,{\rm d}R$) are integrated from $R = 5.7$ a.u. to the boundary, so they are zero at first. After about 12.0 fs, these two probabilities become stable, although the probabilities of the lower state ψ_g and upper state ψ_u are still changing (Fig. 3(c)). This is because the phases of two wavefunctions $\psi_{\rm r}$ and $\psi_{\rm l}$ are still affected by the THz pulse. When the THz pulse ends, the oscillations of the states ψ_g and ψ_u will also stop.

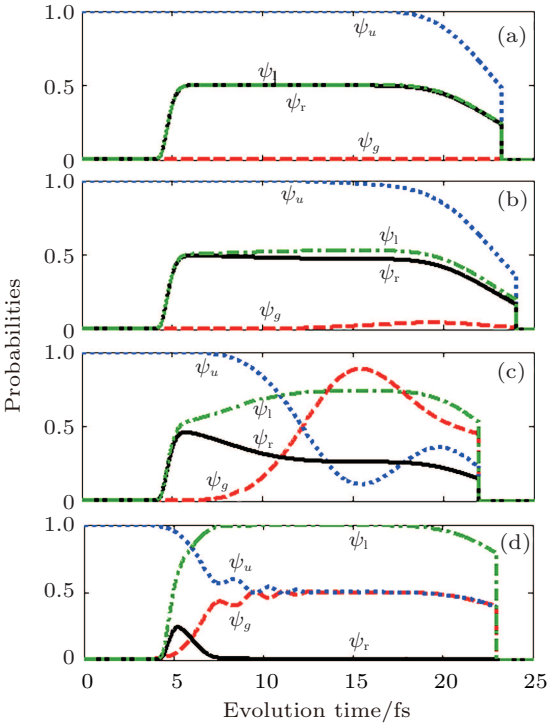


Fig. 3. (color online) Results of electron probabilities on the ψ_g, ψ_u, $\psi_{\rm l}$, and $\psi_{\rm r}$ states, calculated from the coupled equations. The time delay between the pre-excited Gaussian-type wave packet and the THz pulse dt = 21.4 fs. The peak intensities of the THz pulse are 3.8×10^6, 3.8×10^8, 3.8×10^{10}, and 3.8×10^{12} W/cm^2, respectively. After about 18 fs, the nuclear wave packet reaches the boundary and is absorbed by the mask.

What causes the distortions of curve A in Fig. 2(a)? To answer this question, we investigate the time-dependent electron probabilities of different parts: PD_+ (PD_-) for the probability of an electron being localized on the right (or left) proton, PG for the electron probability of high vibrational bound states, $PGI_\pm$ and $PI_\pm$ for the ionized electrons of the six sections, respectively, as indicated in Fig. 4.

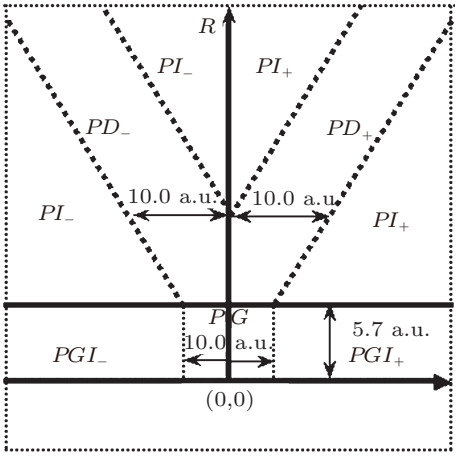


Fig. 4. Time-dependent electron probabilities of different regions.

Figures 5(a1), 5(b1), and 5(c1) show the snapshots of the common logarithm of the electron–nuclear probability density distribution taken at the end of the simulation ($t_{\rm end} = 85.3$ fs) with the time delays $\Delta t = 10.0$, 20.0, and 29.4 fs, respectively. From these figures, one can find that the electrons are excited not only onto the 2p σ_u state, but also onto the higher 3s σ state. The temporal evolutions of the electron probabilities of different parts are presented in Figs. 5(a2), 5(b2), and 5(c2), where the integrations for $PD_{\pm}$ start from $R = 5.7$ a.u. When $\Delta t = 10.0$ fs, the dissociation starts at $t = 17.9$ fs. In this case, the electric field of the THz pulse is close to zero when electrons are excited and the following electric force is in the right direction. From Fig. 5(a2), one can find that many electrons on the right proton are ionized before the dissociation (PI_+). Finally, we can obtain $P_+ = 0.020$, $P_- = 0.143$, and the dissociation asymmetry parameter $A = -0.755$.

In the case of $\Delta t = 20.0$ fs, the dissociation process starts at $t = 27.9$ fs and the whole dissociation process happens around the crest of the THz electric field. Following the above analysis, more electrons on the right proton (PD_+) should be forced to move into the left one (PD_-) by higher intensity steering pulse. But in Fig. 5(b2), PD_+ is just a little larger than PD_- finally. This is because the THz electric field is strong when the electron is excited by the UV pulse. The dressing of the strong THz pulse reduces the energy of the 3s σ state of the right proton and makes the 3-photon resonance possible. Some of the electrons on the right proton are excited onto the higher 3s σ state, which dramatically damages the electron localization. The damage to the asymmetry parameter around $\Delta t = 42.7$ fs in Fig. 2(a) is caused by the same reason. In the case of Fig. 5(a2), the intensity of the THz pulse is not strong enough to induce a similar process.

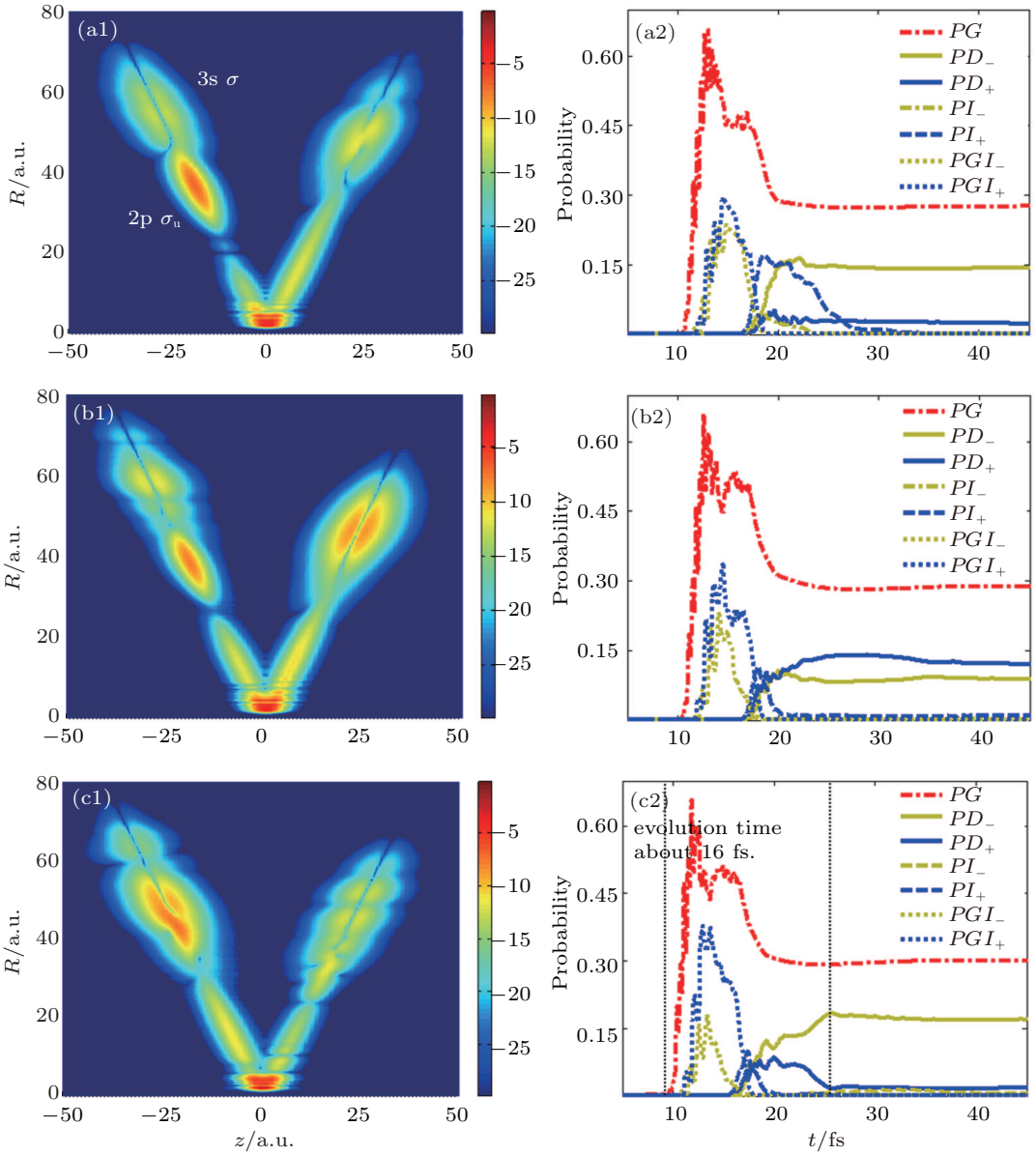


Fig. 5. (color online) Snapshots of the common logarithm of the electron–nuclear probability density distribution taken at $t_{\rm end} = 85.3$ fs for time delays 10.0 fs (a1), 20.0 fs (b1), and 29.4 fs (c1) (right column), and their time-dependent electron probabilities of $PD_{\pm}(t)$, $PI_{\pm}(t)$, $PG(t)$, and $PGI_{\pm}(t)$ (left column).

In the case of $\Delta t = 29.4$ fs, the dissociation process starts at $t = 37.3$ fs, where the field strength of the THz pulse is larger than that of Fig. 5(a2), but smaller than that of Fig. 5(b2). At first, the ionization of the electron on the right proton (PI_+) makes PD_+ a little smaller than PD_-. After the reverse of the direction of the THz electric field at $t = 42.6$ fs, more electrons are pulled from the right proton (PD_+) to the left one (PD_-). Finally, we can obtain $PD_+ = 0.017$, $PD_- = 0.167$, and the dissociation asymmetry parameter $A = -0.815$, as shown in Fig. 5(c2).

If the peak intensity of the UV pulse is small, e.g., 7.1×10^{13} W/cm^2, the total dissociation ratio will be low and the total ionization probability will be close to zero. More importantly, almost no electron is excited onto the higher 3s σ state, which is caused by a 3-photon resonance process and depends on the dressing of the THz pulse dramatically. Then the THz pulse can control the motion of the excited electron more efficiently. The curve A will be more similar to the simulation result of the coupled equation (Fig. 2(b)), as shown in Fig. 6.

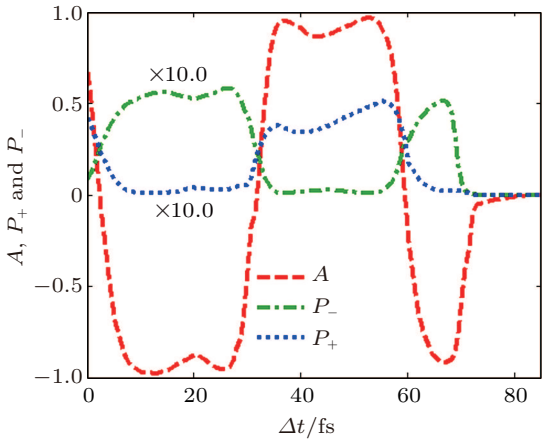


Fig. 6. (color online) The same as Fig. 2(a) except that the peak intensity of the UV pulse is 7.1×10^{13} W/cm^2, the ionization probability is near zero, so it is not plotted here.

4. Summary

We demonstrate that the electron localization control in the dissociation of H_2^+ can be achieved by using the two laser pulses in UV and THz spectral regimes. The results show that the electron localization depends on the direction of the THz pulse and the intensities of the UV and THz pulses. When the peak intensity of the UV pulse is low, the total ionization probability is near zero and the dissociative process can be efficiently controlled by the THz pulse. A high asymmetry parameter can be obtained, although the total dissociation probability is low. If the peak intensity of the UV pulse is high, the total dissociation ratio will be large and more electrons will be ionized. More importantly, some electrons will be excited onto the higher 3s σ state by a 3-photon resonance process. In this case, a high asymmetry parameter can be obtained only at some special time delay. So if one wants to obtain a high asymmetry parameter, the half period of the steering pulse should match the effective time of the molecular dissociation, which is about 16.0 fs for the dissociation of H_2^+.

References

[1] Brixner T and Gerber G 2003 *Chem. Phys. Chem.* **4** 418
[2] Lan P, Lu P, Cao W, Li Y and Wang X 2007 *Phys. Rev. A* **76** 011402
[3] González Castrillo A, Palacios A, Bachau H and Martín F 2012 *Phys. Rev. Lett.* **108** 063009
[4] Zewail A H 2000 *J. Phys. Chem. A* **104** 5660
[5] Babrec T and Krausz F 2000 *Rev. Mod. Phys.* **72** 545
[6] Lindner F, Schätzel M G, Walther H, Baltuška A, Goulielmakis E, Krausz F, Milošević D B, Bauer D, Becker W and Paulus G G 2005 *Phys. Rev. Lett.* **95** 040401
[7] Roudnev V, Esry B D and Ben Itzhak I 2004 *Phys. Rev. Lett.* **93** 163601
[8] Kling M F, Siedschlag Ch, Verhoef A J, Khan J I, Schultze M, Uphues Th, Ni Y, Uiberacker M, Drescher M, Krausz F and Vrakking M J J 2006 *Science* **312** 246
[9] Chelkowski S, Yudin G L and Bandrauk A D 2006 *J. Phys. B: At. Mol. Opt. Phys.* **39** S409
[10] Znakovskaya I, von den Hoff P, Marcus G, Zherebtsov S, Bergues B, Gu X, Deng Y, Vrakking M J J, Kienberger R, Krausz F, de Vivie-Riedle R and Kling M F 2012 *Phys. Rev. Lett.* **108** 063002
[11] Geppert D, vonden Hoff P and de Vivie-Riedle R 2008 *J. Phys. B: At. Mol. Opt. Phys.* **41** 074006
[12] Roudnev V and Esry B D 2007 *Phys. Rev. Lett.* **99** 220406
[13] McKenna J, Anis F, Sayler A M, Gaire B, Nora G Johnson, Parke E, Esry K D, Carnes B D and Ben Itzhak I 2012 *Phys. Rev. A* **85** 023405
[14] Fischer Bettina, Kremer Manuel, Pfeifer Thomas, Feuerstein Bernold, Vandana Sharma, Uwe Thumm, Claus Dieter Schröter, Robert Moshammer and Joachim Ullrich1 2010 *Phys. Rev. Lett.* **105** 223001
[15] He F 2012 *Phys. Rev. A* **86** 063415
[16] Kling M F, Siedschlag Ch, Znakovskaya I, Verhoef A J, Zherebtsov S, Krausz F, Lezius M and Vrakking M J J 2008 *Mol. Phys.* **106** 455
[17] Hirori H, Doi A, Blanchard F and Tanaka K 2011 *Appl. Phys. Lett.* **98** 091106
[18] Alexander Sell, Alfred Leitenstorfer and Rupert Huber 2008 *Opt. Lett.* **33** 2767
[19] Christoph P Hauri, Clemens Ruchert, Carlo Vicario and Fernando Ardana 2011 *Appl. Phys. Lett.* **99** 161116
[20] Xie X, Dai J M and Zhang X C 2006 *Phys. Rev. Lett.* **96** 075005
[21] Bai Y, Song L W, Xu R J, Li C, Peng L, Zeng Z N, Zhang Z X, Lu H H, Li R X and Xu Z Z 2012 *Phys. Rev. Lett.* **108** 255004
[22] Wu J, Tong Y Q, Li M, Pan H F and Zeng H P 2010 *Phys. Rev. A* **82** 053416
[23] Jia Z G, Zeng Z N, Li R X, Xu Z Z and Deng Y P *Phys. Rev. A* **89** 023419
[24] Zheng Y H, Zeng Z N, Li R X and Xu Z Z 2012 *Phys. Rev. A* **85** 023410
[25] Chelkowski Szczepan, André D Bandrauk, André Staudte and Corkum Paul B 2007 *Phys. Rev. A* **76** 013405
[26] Wang Y S and Xu Z Z 2000 *Chin. Phys. Lett.* **17** 491
[27] Chen C Z, Zhou X X and Cao W J 2011 *Acta Phys. Sin.* **60** 054210 (in Chinese)
[28] Chen J G, Yu X P, He L J, Xu Y Y and Yang Y J 2011 *Acta Phys. Sin.* **60** 053206 (in Chinese)
[29] Zeng Z N, Li R X, Yu W and Xu Z Z 2002 *Chin. Phys. Lett.* **19** 1112
[30] Zeng Z N, Li R X, Yu W and Xu Z Z 2003 *Phys. Rev. A* **67** 013815
[31] Liu K L, Hong W Y, Zhang Q B and Lu P X 2011 *Opt. Express* **19** 26359
[32] He F, Ruiz Camilo and Becker Andreas 2007 *Phys. Rev. Lett.* **99** 083002
[33] Fleischer Sharly, Zhou Y, Robert W Field and Nelson Keith A 2011 *Phys. Rev. Lett.* **107** 163603